

Article

Experimental Investigation on Cement Mortar Bricks Manufactured with Fennel Wastes

Antonio Formisano * and Antonio Davino 

Department of Structures for Engineering and Architecture, University of Naples "Federico II",
Piazzale Vincenzo Tecchio 80, 80125 Naples, Italy; davino.ad@gmail.com

* Correspondence: antoform@unina.it

Abstract: Current practices supporting sustainable building design aim at reducing the expenditure of natural resources, such as raw materials, energy and water, in the production of construction supplies. In the current paper water is replaced by fennel centrifugate (FC) for the realization of cement mortar bricks. After having identified the most suitable cementitious pre-mixed over three potential candidates, the mechanical and physical characteristics of the FC bricks are compared to cement mortar bricks, prepared with regular water, by means of bending, compression at ordinary and high temperatures, imbibition and acoustic tests. From compared results, it is noticed that FC bricks have the same imbibition property, but tensile and compression (ordinary and high temperatures) resistances have about 20% less than the control specimen ones. The acoustic tests revealed a better response of FC bricks to the high frequencies greater than 1600 Hz. However, fennel fibres do not provide a manifest advantage, likely due to the small size of the centrifuged fragments that are not able to enhance the product tensile resistance.

Keywords: sustainable building; reuse; fennel wastes; cement mortar; green bricks



Citation: Formisano, A.; Davino, A. Experimental Investigation on Cement Mortar Bricks Manufactured with Fennel Wastes. *Buildings* **2022**, *12*, 230. <https://doi.org/10.3390/buildings12020230>

Academic Editor: Luca Pelà

Received: 18 January 2022

Accepted: 14 February 2022

Published: 17 February 2022

Publisher's Note: MDPI stays neutral with regard to jurisdictional claims in published maps and institutional affiliations.



Copyright: © 2022 by the authors. Licensee MDPI, Basel, Switzerland. This article is an open access article distributed under the terms and conditions of the Creative Commons Attribution (CC BY) license (<https://creativecommons.org/licenses/by/4.0/>).

1. Introduction

The construction industry has a significant adverse impact on the environment, with serious worldwide implications. The European industry accounts for about 46% of the annual construction and demolition waste (CDW) according to Eurostat [1]. Similarly, the U.S. building industry contributes with 25% of non-industrial waste generation per year [2]. In China, the CDW reaches 30–40% of the total waste and recycling represents less than 5% [3]. From an environmental perspective, this category employs an enormous quantity of resources, including raw materials, energy and water [4–6]. The first are the focus of many researchers, which aim at recycling the building elements, either as isolated items or as components of novel products [7]. Several natural fibres, such as hemp, flax, jute and sisal, are currently being employed in fibre-reinforced composites [6], whose manufacturing method was widely investigated in literature [8–14].

Less attention has been paid to the use of water in the building industry, besides single case-studies, often performed in desertic or semi-desertic regions. Mekonnen and Hoekstra [15] reported that the overall trade of international virtual water (embodied in the production of food, fibre and non-food commodities) equals 26% of global water footprint. In particular, construction consumes 16% of the water, worldwide [7]. For what concerns the Mediterranean basin, the water availability is scarce and mainly based on mountain runoff water (50–90%) [16,17]. Thus, it is fundamental to preserve the water amount and quality, thereby safeguarding the accessible resources [18]. To this regard, the project aims at employing alternative plant-derived water sources in bricks manufacturing. The fennel (*Foeniculum vulgare*) bulb contains about 90 g of water per 100 g of raw product [19]. It is a biennial plant originating from southern Europe and, more generally, from the Mediterranean region. Nowadays, it is being cultivated worldwide due to its broad use [20].

In fact, fennel is employed in medicine [21–24], animal nutrition [25,26], pharmaceuticals, cosmetics [27] and fashion industry [28]. Most importantly, fennel plantations can be grown in arid- and semi-arid regions of the planet [29]. In the production chain, the outermost rigid leaves are usually discarded for being too hard and fibrous. This selection results in the disposal of about 30% of the overall production for a total of around 70,000 tons per year only in the Southern regions of Italy [30].

The innovative pipeline presented by the paper aims at reducing the use of water in cement production by substituting it with water contained in fennel by-products. In this context, fennel centrifugate (FC) was employed as additive to cement mortars for bricks manufacturing. The experimental campaign consists in a preliminary investigation that intends to identify, among three types, the most suitable cement mortar. The compression and bending tests, as well as the economic evaluation, revealed the most appropriate type for the aims of this research. Consequently, a detailed characterization of the manufactured bricks was performed to evaluate potential physical and mechanical benefits provided by the supplement of fennel fibres. The investigations include bending, compression (at ordinary and high temperatures), soaking and acoustic tests.

In accordance with the Green Building Challenge process, the current work aims at: (1) reducing waste by employing a by-product of the agricultural industry, (2) employing less water in the process of cement-making by using fennel-centrifugate instead, (3) testing a new source of natural fibres (fennel), which are widely produced on the Italian territory and (4) fostering the use of local goods.

2. Materials and Methods

2.1. Experimental Setup

The experimental setup is summarized in the flow chart of Figure 1. Organization of work steps was done based on consultation of appropriate literature papers [31,32]. Briefly, a preliminary investigation was performed to settle the most suitable binding agent for a novel fennel-based composite material (phase I). After having defined the water content of fennel (%), three cement mortars (A, B and C) were tested. A total of 36 samples (see Section 2.3.1) were employed. The most appropriate combination was determined with compression and bending tests. Hence, a detailed physical and mechanical characterization of the obtained bricks was performed (phase II). For that, two sets of samples were prepared: (I) 24 parallelepiped samples for bending, compression and shrinkage tests. Four of these samples were cut and reshaped into 6 equally sized bricks and employed for imbibition and high temperature compression tests; (II) 12 cylindrical samples for acoustic tests (see Section 2.3.2).

2.2. The Fennel Water Content

Fennel leaves were centrifuged to obtain the fennel centrifugate (FC) and weighted on a precision balance (Wunder ACS-3M, Trezzo sull'Adda (Milan), Italy). The blend was placed in a muffle oven (FM22, Falc Instruments, Treviglio (Bergamo), Italy) at 105 °C for about 10 min to eliminate the water fraction and repeatedly weighted, until stabilization. The final weight of the dried samples was employed to calculate the fennel 'dry' mass (fibres, carbohydrates, lipids, calcium and vitamins) and the percentage of water. The same procedure was applied to the edible part of fennel.

2.3. Sample Preparation

All samples were prepared according to the UNI EN 196-1:2016 guidelines [33].

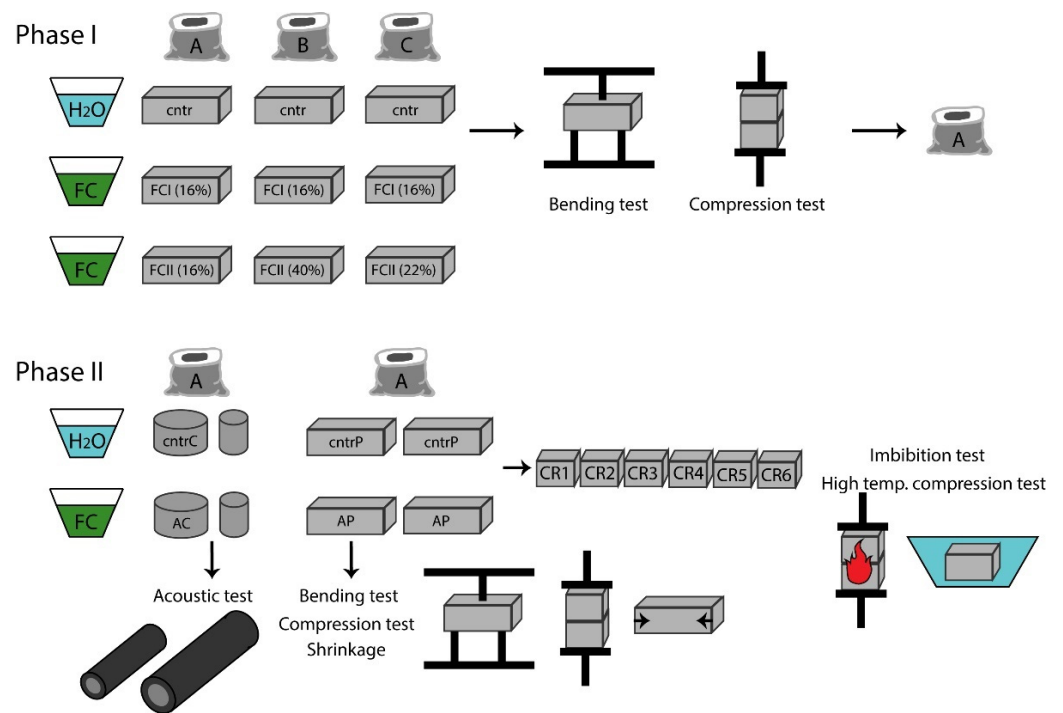


Figure 1. Overview of the experimental setup.

2.3.1. Phase I Samples

A total of 36 samples (Table 1, Figure 1) were prepared with one of three commercial cement mortars. Each matrix was combined with either water or FC to cast the following set of samples: (I) Control samples (cntr): 4 specimens/mortar. These samples were prepared by adding 16% tap water to the appropriate cement powder; (II) FC I: 4 specimens/mortar. In this case, exclusively the water obtained from fennel centrifugation was employed. To have a solid comparison between the obtained products, a fixed percentage (16%) was chosen. Such percentage was defined as the smallest value among the producers' indications of each cement matrix; (III) FC II: 4 specimens/mortar. The samples were prepared by replacing the percentage of water indicated by the producers with FC (16% for mortar A, 40% for B and 22% for C) (Figure 2).

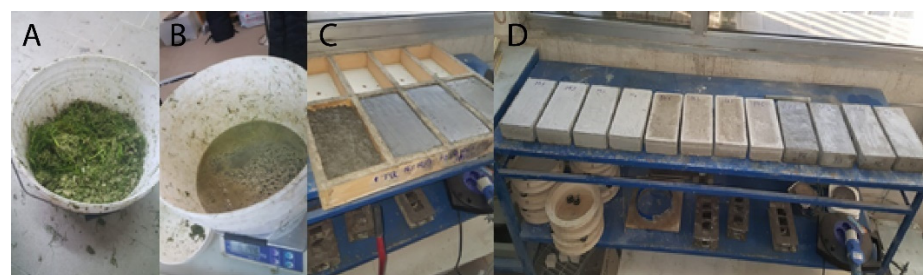


Figure 2. Preparation of FC (A,B) and casting of phase I specimens (C,D).

The casted samples were employed for compression tests. The two obtained fragments were reshaped and consequently joined with a high-strength cement mortar. The latter has mechanical characteristics superior to that used for the realization of the samples object of this research.

Table 1. Samples casted in phase I with 6 fennel-mortar combinations (cntr: control samples (mortar + tap water); FC I: mortar and 16% fennel centrifugate; FC II: mortar and variable % of fennel centrifugate).

	Cement Mortar		
	A	B	C
Control (16% H ₂ O)	cntrA1	cntrB1	cntrC1
	cntrA2	cntrB2	cntrC2
	cntrA3	cntrB3	cntrC3
	cntrA4	cntrB4	cntrC4
FC I (16% fennel centrifugate)	FCI_A1	FCI_B1	FCI_C1
	FCI_A2	FCI_B2	FCI_C2
	FCI_A3	FCI_B3	FCI_C3
	FCI_A4	FCI_B4	FCI_C4
FC II (variable % fennel centrifugate)	FCII_A1	FCII_B1	FCII_C1
	FCII_A2	FCII_B2	FCII_C2
	FCII_A3	FCII_B3	FCII_C3
	FCII_A4	FCII_B4	FCII_C4

2.3.2. Phase II Samples

Twenty-four parallelepiped-shaped specimens (Table 2) were prepared for shrinkage, bending and compression tests and 8 cylindrical specimens (Table 3), with 2 different diameters (98 mm for 4 blocks and 24 mm for other 4 blocks), for acoustic tests. The dimensions of this second group were dictated by the experimental setup for acoustic analyses, which require the insertion of the cylinders in steel tubes for impedance tests. The small and large diameters are required to investigate both low- and high-frequency acoustic waves. All samples (Figure 3) were prepared using mortar A and 16% fennel centrifugate instead of regular water, in accordance with the supplier's instructions. Tables 2 and 3 report the sample acronyms and dimensions, as well as the casting and dismantling dates.

Table 2. Parallelepiped (P)-shaped specimens for phase II (cntr: control samples, mortar A + water; AP: mortar A + fennel centrifugate bricks).

Acronym	Casting Date	Dimensions		Dismantling Date
		Length (mm)	Depth (mm)	
cntrP1	07/08/2019	250	120	17/09/2019
cntrP2	07/08/2019	250	120	17/09/2019
cntrP3	07/08/2019	250	120	17/09/2019
cntrP4	07/08/2019	250	120	17/09/2019
cntrP5	24/10/2019	250	120	19/11/2019
cntrP6	24/10/2019	250	120	19/11/2019
cntrP7	24/10/2019	250	120	19/11/2019
cntrP8	24/10/2019	250	120	19/11/2019
cntrP9	24/10/2019	250	120	19/11/2019
cntrP10	24/10/2019	250	120	19/11/2019
AP1	07/08/2019	250	120	17/09/2019
AP2	07/08/2019	250	120	17/09/2019
AP3	07/08/2019	250	120	17/09/2019

Table 2. *Cont.*

Acronym	Casting Date	Dimensions		Dismantling Date
		Length (mm)	Depth (mm)	
AP4	07/08/2019	250	120	17/09/2019
AP5	07/08/2019	250	120	17/09/2019
AP6	07/08/2019	250	120	17/09/2019
AP7	07/08/2019	250	120	17/09/2019
AP8	07/08/2019	250	120	17/09/2019
AP9	07/08/2019	250	120	17/09/2019
AP10	07/08/2019	250	120	17/09/2019
AP11	07/08/2019	250	120	17/09/2019
AP12	07/08/2019	250	120	17/09/2019
AP13	07/08/2019	250	120	17/09/2019
AP14	07/08/2019	250	120	17/09/2019

Table 3. Cylindrical (C)-shaped specimens for phase II (cntr: control samples, mortar A + tap water; AC: mortar A + fennel centrifugate bricks).

Acronym	Casting Date	Shape		Dismantling Date	Weight (g)
		Diameter (mm)	Height (mm)		
cntrC1	09/01/2020	98	50	22/01/2020	724
cntrC2	09/01/2020	98	48	22/01/2020	692
cntrC3	09/01/2020	98	55	22/01/2020	738
cntrC4	09/01/2020	28	51	22/01/2020	61
cntrC5	09/01/2020	28	51	22/01/2020	63
cntrC6	09/01/2020	28	50	22/01/2020	63
AC1	09/01/2020	98	49	22/01/2020	680
AC2	09/01/2020	98	52	22/01/2020	701
AC3	09/01/2020	98	51	22/01/2020	711
AC4	09/01/2020	28	51	22/01/2020	59
AC5	09/01/2020	28	52	22/01/2020	64
AC6	09/01/2020	28	49	22/01/2020	59

**Figure 3.** Centrifugation of fennel side-products (A) and preparation of cylindrical bricks for acoustic tests (B).

Two P-shaped control and two P-shaped fennel bricks were cut into 6 equally sized specimens (Table 4) for high temperature compression and imbibition tests.

Table 4. Cutting and reshaping of specific samples for high temperature compression and imbibition tests (cntr: control samples, mortar A + tap water; AP: mortar A + fennel centrifugate bricks).

Original Sample	Cut and Reshaped (C/R) Samples					
cntrP4	cntrP4_CR1	cntrP4_CR2	cntrP4_CR3	cntrP4_CR4	cntrP5_CR5	cntrP6_CR6
cntrP10	cntrP10_CR1	cntrP10_CR2	cntrP10_CR3	cntrP10_CR4	cntrP10_CR5	cntrP10_CR6
AP10	AP10_CR1	AP10_CR2	AP10_CR3	AP10_CR4	AP10_CR5	AP10_CR6
AP14	AP14_CR1	AP14_CR2	AP14_CR3	AP14_CR4	AP15_CR5	AP16_CR6

2.4. Testing Activities

The physical and mechanical tests (Section 2.4.1, Section 2.4.2, Section 2.4.3, Section 2.4.4, and Section 2.4.5) were carried out in the laboratory of the Department of Structures for Engineering and Architecture (DIST), Naples. The acoustic tests were entrusted to the company “Innovacustica Srl”, Alvignano (Caserta, Italy) and performed at the laboratories located in in Casalnuovo di Napoli, Italy.

2.4.1. Bending Tests

Three-points bending tests were carried out with a 500 kN MTS 810 Universal Machine (Germany), as regulated by UNI EN 12390-5:2019 [34]. All 36 phase I- and 9 phase II-samples (3 cntr- and 6 FC-bricks) were tested for potential use in seismic areas. A concentrated force (loading speed $v = 0.005$ MPa/s) was applied in the middle of the specimen, which was constrained at the ends by two cylindrical supports. The distance between the support pins was 150 mm and the samples were perfectly centred inside the testing machine (Figure 4). In addition to measuring the displacement of the upper loading tool, a transducer located under the specimen reported the downward shift of the brick (Figure 4).



Figure 4. Setup for the three-points bending test.

The flexural strength f_{cf} was calculated with the following equation:

$$f_{cf} = \frac{3 \times F \times L}{2 \times d_1 \times d_2^2} \quad (1)$$

where F is maximum applied load, L is distance between the support pins, d_1 is the specimen's length and d_2 is the specimen's depth.

2.4.2. Compression Tests

The compression tests were carried out with a 500 kN MTS 810 Universal Machine (Germany), as regulated by the UNI EN 12390-3:2019 [35] standards for bricks (Figure 5). The top plate was designed to automatically align with the specimen. The load was increased at a speed of 50 N/s. The compressive strength was calculated by dividing the measured breaking load by the sample's cross-sectional area.



Figure 5. Setup for compression tests.

2.4.3. Shrinkage Tests

Shrinkage of control- and FC-bricks was calculated by measuring the dimensions at the dismantling date and after drying (28 days after dismantling), as regulated by UNI 11307:2008 [36].

2.4.4. Compression Test at High Temperatures

The samples were preheated at 200 °C and 600 °C in a muffle oven (FM22, Falc Instruments, Treviglio, Italy) prior to regular compression tests (as described in Section 2.4.2). The purpose is to evaluate the influence of high temperatures on the mechanical performances of samples by simulating a fire scenario. A pilot test was carried out to identify the procedure timing and potential temperature fluctuations. Three heating cycles were carried out on the cntrP4_CR1 specimen. The following thermoelectric probes were prepared (Figure 6A): (I) T1, inserted inside the specimen to a depth of 5 mm; (II) T2, inserted inside the specimen to a depth of 25 mm; (III) T3, inserted in the oven for the acquisition of the contact temperature. The data acquisition continued outside the oven to gain the cooling trend of the bricks. To reproduce the most realistic conditions and evaluate the cooling resulting from contact with the compression press, the pilot specimen was extracted from the oven and placed between two steel plates. Thus, it was possible to infer the temperature at which the brick fails under the compression test (Figure 6B).

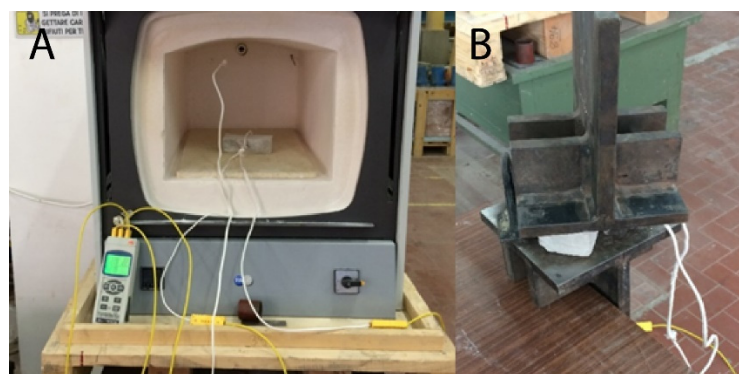


Figure 6. Thermoelectric probes for temperature monitoring (A) and temperature acquisition after extraction from the oven (B).

Figure 7 reports the pilot test with preheating at 600 °C. A temperature drop is observed after 102 min due to a voluntary opening of the oven. This was conceived to estimate the time required to restore the set temperature after extracting a sample.

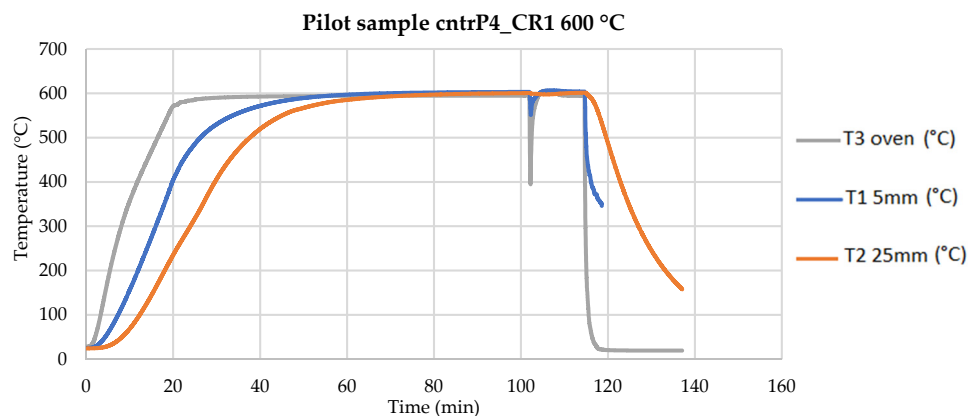


Figure 7. Pilot test at 600 °C.

2.4.5. Soaking Tests

In order to evaluate the amount of water absorbed by the bricks, they were placed under water for two weeks. Weight measurements were performed every 24 h [37].

2.4.6. Acoustic Tests

Transmission loss (TL) measurements were carried out using impedance tubes (Kundt tubes), according to the technical standard ASTM E2611-09 [38]. The instruments are listed in Table 5.

Table 5. Instruments employed to measure transmission loss.

Type	Model	Description
4 channels impedance tubes	BSWA SW 422	100 mm diameter tube with loudspeaker and 100 mm extension tube
4 channels impedance tubes	BSWA SW 477	30 mm diameter tube with loudspeaker and 30 mm extension tube
Microphones	BSWA MPA416	n. 4 1/4" microphones
Power Amplifier	BSWA TECH PA50	Power amplifier and signal generator
Sound card	BSWA TECH MC3242	4 channels DAQ Card
Sound calibrator	BSWA CA115	1000 Hz 114 dB sound calibrator

The investigated frequency range was 63–6300 Hz. The impedance tubes with diameters of 30 mm and 100 mm (Figure 8) covered, respectively, a complete range of 63–1800 Hz and 800–6300 Hz. In particular, the tube with a larger diameter was used for low frequencies, and the one with a smaller diameter was used for high frequencies.

The samples were intentionally casted with diameters smaller than the impedance tube to be coated with insulating material before insertion. The purpose was both to preserve the pipe from scratches and to create a layer of sound insulation between the mortar surface and the rigid surface of the steel pipe.

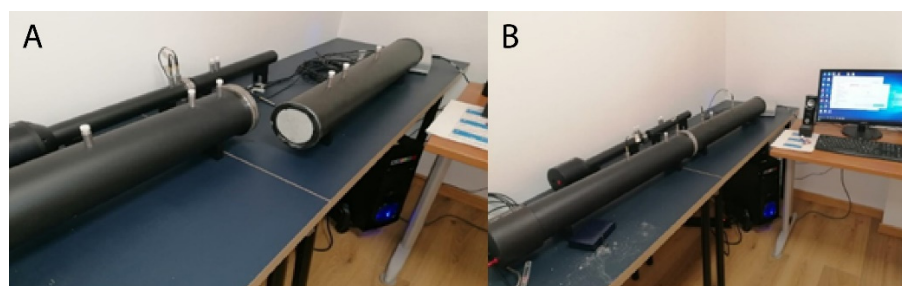


Figure 8. BSWA SW 422 and BSWA SW477 impedance tubes: (A) sample loading; (B) data acquisition.

3. Results

3.1. Phase I: Identifying the Ideal Fennel-Mortar Combination

3.1.1. Percentage of Water in Fennel Centrifugate (FC)

The centrifugate of fennel leaves was weighted in duplicate: FC1 (gross weight: 189.04 g) and FC2 (gross weight: 189.36 g). After incubation at 105 °C, the dried weights equalled 5.96 g and 5.99 g, respectively. Thus, the ‘dry’ mass corresponded to 7.5% of the fennel centrifugate and the water fraction to 92.5%. Concerning the edible part of fennel, 2.2 g of water-free mass were obtained for 100 g of starting material. The percentage of water-free mass (mainly fibres) was in line with the chemical composition tables of fennel [21]. The observed reduction possibly depended on the high content of fibres of the outer fennel leaves.

3.1.2. Flexural Strength Tests

The results in terms of flexural stress are summarized in Table 6. The specimens manufactured with mortar A or mortar B and 16% FC did not show great differences in terms of resistance compared to the control specimens. The greatest reduction in resistance was observed for mortar C. The overall best performances were registered for bricks prepared with the mortar A.

Table 6. Results of three-point bending flexural test in terms of flexural stress. The average values are reported with the standard deviation (SD).

Sample		Mortar A		Mortar B		Mortar C	
		Stress (MPa)	Average \pm SD (MPa)	Stress (MPa)	Average \pm SD (MPa)	Stress (MPa)	Average \pm SD (MPa)
Control (16% H ₂ O)	1	4.14		2.34		6.72	
	2	3.11	3.39 \pm 0.43	3.72	2.77 \pm 0.55	4.65	5.76 \pm 1.00
	3	3.16		2.53		6.79	
	4	3.16		2.50		4.86	
FC I (16% fennel centr.)	1	2.95		4.20		1.18	
FC I (16% fennel centr.)	2	3.57	3.30 \pm 0.42	2.00	2.81 \pm 1.03	1.47	1.35 \pm 0.12
	3	2.83		3.40		1.45	
	4	3.83		1.65		1.29	
	FC II (variable % fennel centr.)	1		2.52		1.50	
2		1.86	2.36 \pm 0.39	0.96	1.05 \pm 0.29	0.37	0.29 \pm 0.08
3		2.91		1.04		0.24	
4		2.16		0.69		0.37	

3.1.3. Compression Tests

The results are summarized in Table 7. The highest strength values were obtained with mortar B. The specimens prepared with FC water displayed a drastic reduction in resistance of over 80%. Despite this decrease, for all blocks the average resistance values were greater than 5 MPa, which is the lowest admissible value for employing artificial blocks in the construction of load-bearing walls. This reduction was clearly marked for the samples assembled with mortar C. For mortar A-FC bricks, a 30% drop in resistance was observed with respect to the control specimens.

Table 7. Results of compression tests in terms of tensile strength. The average values are reported with the standard deviation (SD).

Sample		Mortar A		Mortar B		Mortar C	
		Stress (MPa)	Average \pm SD (MPa)	Stress (MPa)	Average \pm SD (MPa)	Stress (MPa)	Average \pm SD (MPa)
Control (16% H ₂ O)	1	17.58		32.48		15.81	
	2	18.73	18.65 \pm 0.65	42.24	36.15 \pm 3.66	19.43	20.03 \pm 3.44
	3	19.31		35.10		19.49	
	4	18.97		34.79		25.41	
FC I (16% fennel centr.)	1	11.40		7.18		1.13	
	2	15.05	12.92 \pm 3.02	10.45	7.87 \pm 3.98	1.58	1.35 \pm 0.23
	3	8.86		12.15		1.58	
	4	16.54		1.71		1.11	
FC II (variable % fennel centr.)	1	14.14		6.16		0.82	
	2	14.14	12.66 \pm 1.83	5.92	6.72 \pm 1.98	0.41	0.58 \pm 0.17
	3	12.73		10.02		0.66	
	4	9.65		4.77		0.44	

Based on the results of bending and compression tests, mortar A was chosen for the assembly of bricks. Thus, greater resistances were measured for mortar A when replacing regular water with fennel centrifugate. Furthermore, the costs of the mortar were lower.

3.2. Phase II: Physical and Mechanical Characterization of the Fennel-Mortara Composite Bricks

3.2.1. Shrinkage Tests

The average dimensions of all samples with the standard deviations are reported in Table 8. With respect to the original size (250 mm \times 120 mm), the results did not show substantial differences in shrinkage between the control- and FC-samples (A).

Table 8. Average and standard deviation (SD) of shrinkage on all tested samples.

Sample	Width \pm SD (mm)	Length \pm SD (mm)
Control	249.0 \pm 0.4	118.0 \pm 0.7
A	249.0 \pm 0.5	119.0 \pm 0.7

Shrinkage is greatly influenced by the relative humidity of the surrounding environment and by the surface-to-volume ratio of the investigated element. Its extent is also conditioned by the installation method and the composition of the mortar, i.e., the water-to-cement ratio and the total amount of cement. An increase in concrete percentage causes an amplification of the phenomenon. It should be noted that shrinkage causes damaging cracks only in hyperstatically linked elements. For elements constrained in an isostatic manner, the damage is absent.

3.2.2. Bending Tests

The bending tests (Table 9) revealed a 21% reduction of the average bending tensile strength Δf_{ctf} for the samples supplemented with fennel centrifugate. The load-displacement and stress-strain (σ - ϵ) diagrams are presented in Figure 9A,B. It should be noted that the results did not show substantial differences between the displacements measured by the transducer and those recorded by the loading tool.

Table 9. Results of bending tests.

Acronym	Speed (mm/s)	Load _{max} (KN)	f_{ctf} (MPa)	Average \pm SD (MPa)	Δf_{ctf} (%)
cntrP1	0.05	4.64	4.37	4.03 \pm 0.32	-
cntrP2	0.01	3.96	3.61		
cntrP3	0.005	4.40	4.12		
AP1	0.005	3.23	3.15	3.19 \pm 0.35	-21.0
AP2	0.005	2.43	2.69		
AP3	0.005	3.23	2.89		
AP4	0.005	4.29	3.14		
AP5	0.005	3.70	3.68		
AP6	0.005	4.10	3.56		

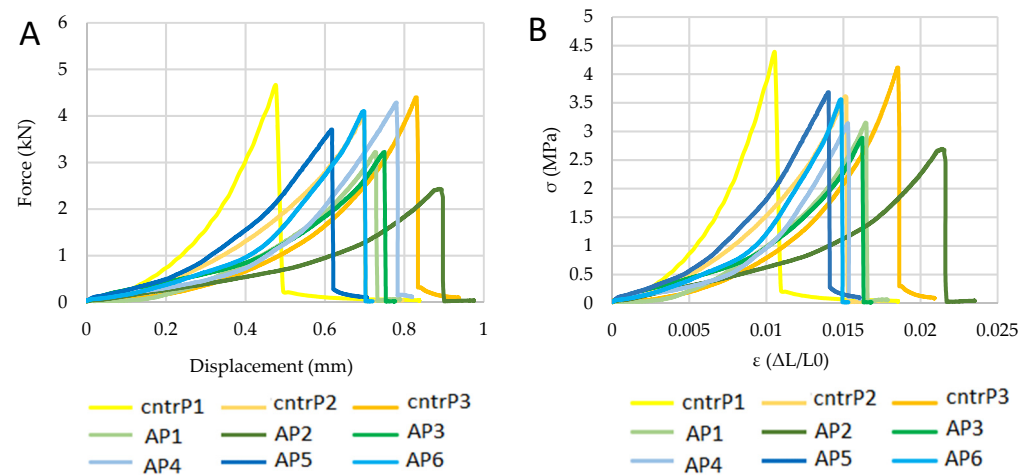


Figure 9. Results of bending tests in terms of load-displacement (A) and stress(σ)–strain(ϵ) (B). Yellow indicates control- and green/blue stands for FC-samples.

3.2.3. Compression Tests

On average, the specimens with additives provided a 17.8% decrease in compressive strength $\Delta \sigma_m$. The results are plotted in Figure 10 and reported in Table 10.

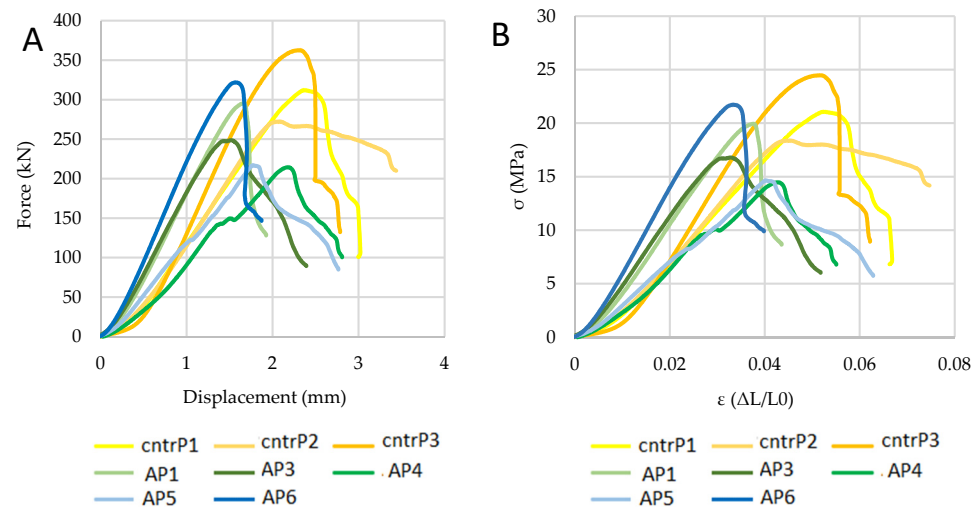


Figure 10. Results of compression tests in terms of load-displacement (A) and stress(σ)–strain(ϵ) (B). Yellow indicates control- and green/blue stands for FC-samples.

Table 10. Results of compression tests.

Acronym	Speed (mm/s)	Load _{max} (KN)	σ (MPa)	Average \pm SD (MPa)	$\Delta\sigma_m$ (%)
cntrP1	0.01	312.08	21.07	21.31 \pm 2.50	-
cntrP2	0.01	272.23	18.38		
cntrP3	0.01	362.68	24.48		
AP1	0.01	295.68	19.96	17.52 \pm 2.89	−17.8
AP3	0.01	248.81	16.80		
AP4	0.01	214.56	14.48		
AP5	0.01	217.09	14.65		
AP6	0.01	321.93	21.73		

3.2.4. Compression Tests at High Temperatures

The results on the 12 specimens, grouped according to the preheating temperature, are reported in terms of flexural stress–strain (σ – ϵ) diagrams in Figure 11. Based on the results obtained during the pilot test, it was possible to calculate the exact temperature of the specimen at both the beginning and the end of the test. The results are summarized in Tables 11 and 12.

Table 11. Overview of compression tests at 200 °C.

Samples at 200 °C							
Sample	T _{sample} (°C)	Δt_{start}	T _{start} (°C)	$\Delta t_{breakage}$	T _{breakage} (°C)	σ_{max} (MPa)	Average \pm SD (MPa)
cntrP4_CR4	193.3	00:00:45	191.2	00:05:35	133.4	17.75	18.07 \pm 0.23
cntrP4_CR2	193.3	00:00:32	192.0	00:06:43	119.8	18.27	
cntrP4_CR5	193.3	00:00:35	191.8	00:05:34	133.7	18.18	
AP10_CR1	193.3	00:00:37	191.7	00:04:09	152.7	13.73	14.68 \pm 0.98
AP10_CR2	193.3	00:00:35	191.8	00:04:06	153.2	14.28	
AP10_CR3	193.3	00:00:38	191.7	00:04:06	153.2	16.02	

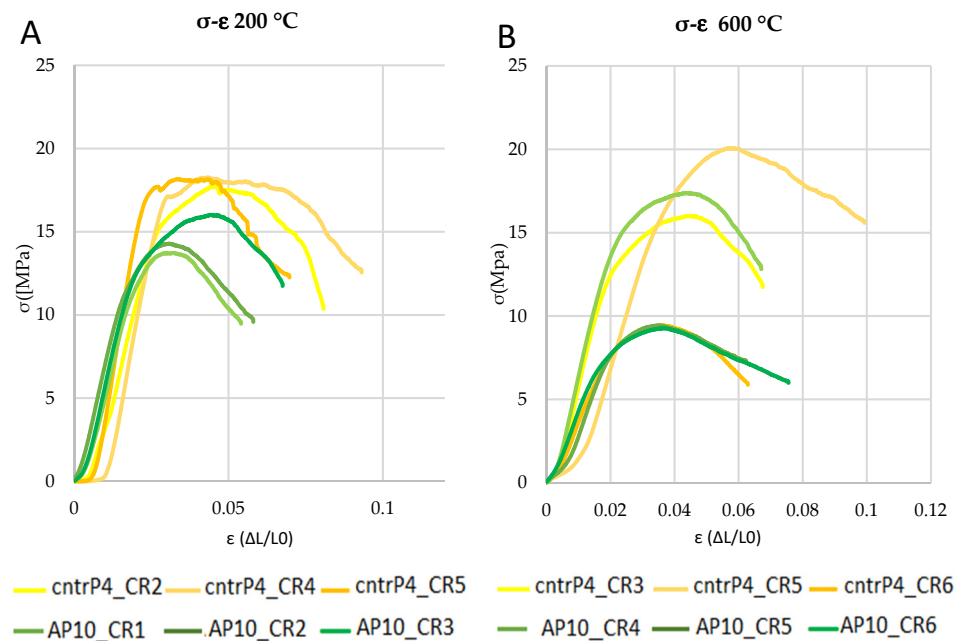


Figure 11. Load-displacement diagrams for samples preheated at 200 °C (A) and 600 °C (B). Yellow indicates control- and green stands for FC-samples.

Table 12. Overview of compression tests at 600 °C.

Samples at 600 °C							
Sample	T _{sample} (°C)	Δt_{start}	T _{start} (°C)	$\Delta t_{\text{breakage}}$	T _{breakage} (°C)	σ_{max} (MPa)	Average \pm SD (MPa)
cntrP4_CR3	601.2	00:00:35	596.5	00:04:36	508.6	16.02	15.18
cntrP4_CR6	601.2	00:00:39	596.5	00:04:27	512.9	9.44	\pm 4.38
cntrP10_CR5	601.2	00:00:45	595.1	00:06:31	447.8	20.07	
AP10_CR4	601.2	00:00:35	596.5	00:04:37	508.6	17.38	12.03
AP10_CR5	601.2	00:00:38	596.5	00:04:23	516.0	9.43	\pm 3.78
AP10_CR6	601.2	00:00:34	597.2	00:05:05	492.5	9.28	

The obtained results were compared with the compression tests at room temperature described in the previous paragraph. The summary diagram of the trends is reported in Figure 12. The temperature decreased by 15% in control specimens and 35% in samples prepared with FC, along with the tension state. The specimens supplemented with FC presented stress values greater than 9 MPa at 600 °C, which overcomes the minimum resistance limit allowed in the seismic area (5 MPa).

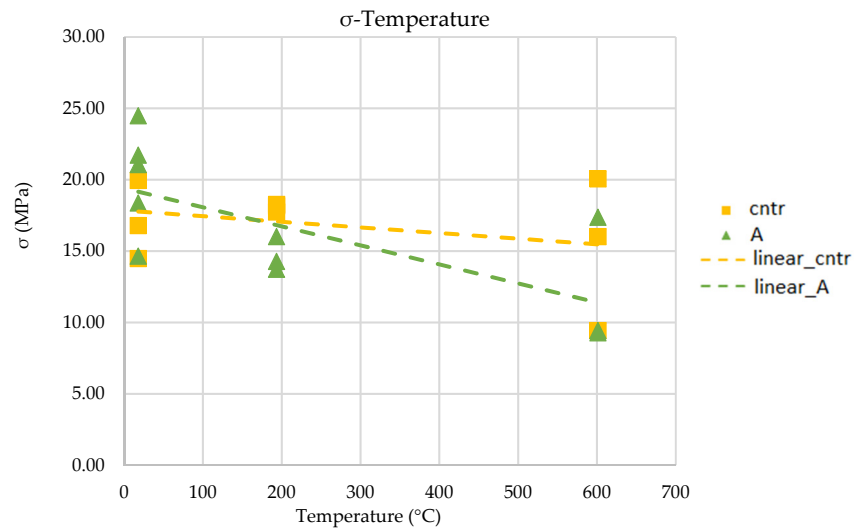


Figure 12. Comparison of test results in terms of compression stress vs. temperature. Yellow indicates control- and green FC-samples.

3.2.5. Soaking Tests

The results show a similar trend for control- and FC-bricks. The initial weight increased by 8% when compared to the initial weight. The plateau was reached after 48 h. Because of the great difference in size, and therefore in weight, the data are plotted in two different graphs (Figure 13).

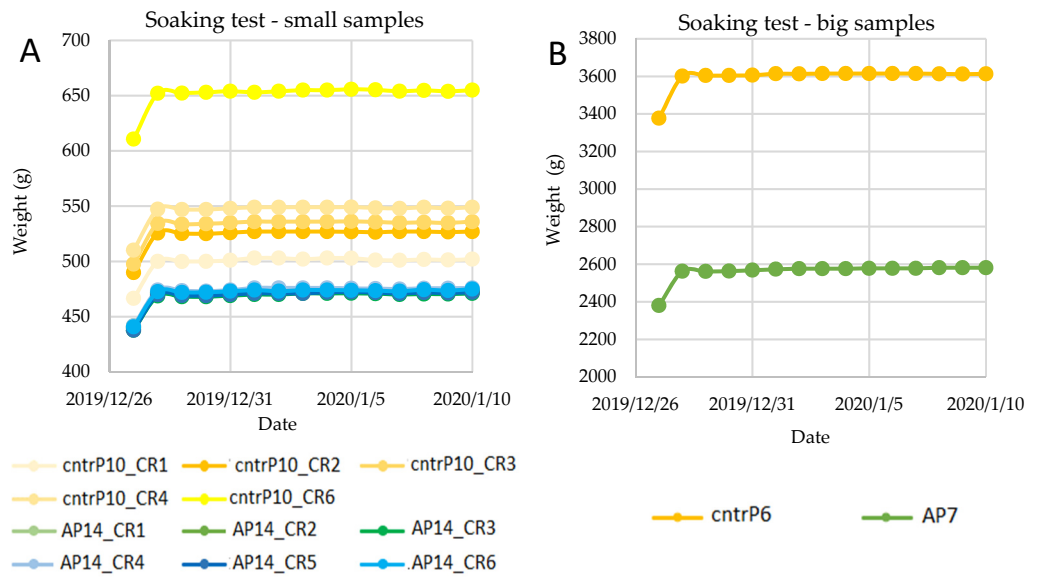


Figure 13. Soaking tests on small (A) and big (B) samples. Yellow indicates control- and green/blue FC-samples.

3.2.6. Acoustic Tests

An increase of sound insulation could be a potential benefit of the fennel fibrous components incorporated into the bricks. Figure 14 reports the transmission loss for all the investigated frequencies for control- and FC-samples.

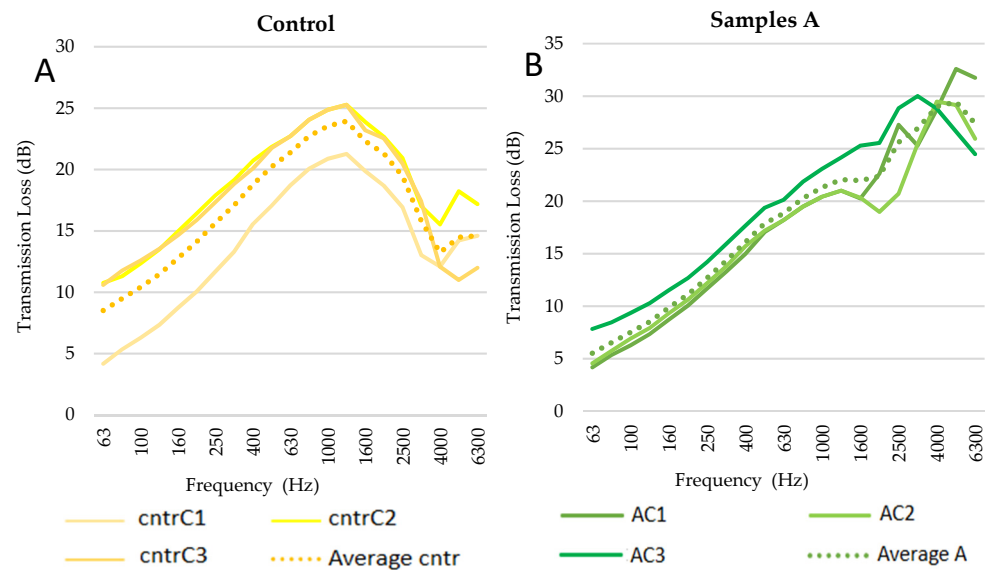


Figure 14. Transmission loss deriving from acoustic tests on control- (A) and FC-bricks (B). Yellow indicates control- and green FC-samples.

The TL curves present a similar trend. However, the curves of control samples are shifted towards higher frequencies, especially sample cntrC1. A possible explanation of this behaviour relies on the irregular circular shape of the specimens, which created gaps between the walls of the tube and the specimens. Future measurements can be improved by further reducing the specimen's diameter and better sealing the edges when inserting the samples into the tubes. To facilitate comparisons between the two groups, the TL averages obtained at each frequency are plotted in a single graph (Figure 15).

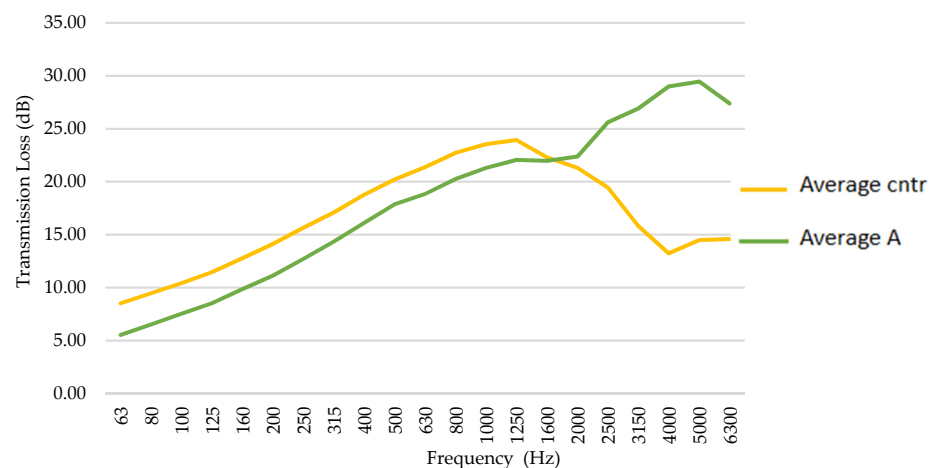


Figure 15. TL averages of control- (yellow) and FC-samples (green) plotted for all the measured frequencies.

At medium-low frequencies, of a major interest in the civil sector [39], the fennel centrifugate bricks display a behaviour comparable to controls. However, it provides a better insulation at higher frequencies.

4. Conclusions and Future Perspectives

The presented work aimed at supporting the use of fennel processing waste in the construction industry. Fennel centrifugate (FC) can be combined with matrices into bricks, which are environmentally sustainable due to the following reasons: (1) water is preserved, as it is replaced by fennel centrifugate; (2) agricultural waste is reduced by giving a second

life to fennel by-products that find less employment in satellite industries; (3) fennel fibres could be employed as additional source of natural fibres in building industry. Furthermore, the use of fennel by-products in building industry is in line with the current directives to prefer the employment of local goods.

The experimental campaign was designed to first identify, among three different mortar-fennel combinations, the most suitable one for the mentioned research objectives. Mortar A was chosen based on the physical and mechanical performances, as well as for the reduced cost. Thus, mortar A was employed for the preparation of a set of samples used in the second phase of testing. The latter was intended to provide a broader picture of the material performance. It was achieved that, for bricks manufactured with 16% of FC instead of water, mortar A is preferable to mortar B because of its significantly greater resistances (almost double). The bricks manufactured with mortar A did not show any significant reduction in size compared to the control specimens and, overall, there was a minimal shrinkage compared to the original dimensions. The bending tests highlighted a 20% reduction of tensile strength in the FC-bricks compared to the control specimens. The samples supplemented with fennel subjected to compression tests displayed a 17.8% resistance reduction compared to control specimens.

The same test performed at high temperature revealed a 15% reduction in compressive strength for the control specimens, which increased to 35% for FC bricks. Nonetheless, in both cases, at 600 °C the values were greater than 9 MPa, which exceeds the minimum resistance limit allowed in seismic areas (5 MPa).

The imbibition tests showed an increase of weight that equals 8% in mass for both control specimens and FC bricks after 24 h. After that period, the weight remained constant over the subsequent 14 days.

The acoustic tests showed that the insulation characteristics of the two types of materials are comparable. In particular, they showed a similar behaviour at low frequencies, which is of greater interest in the civil sector, but a better response at high frequencies.

In conclusion, the paper revealed that the replacement of water by fennel centrifugate for the preparation of cement mortar bricks results in products with performances equivalent to the ordinary mortar bricks. The addition of fibres did not produce evident benefits. This was probably due to the centrifugation process of fennel, which possibly results in too small fragments to give a significant contribution to tensile resistance. For this reason, further developments of the research will be devoted to investigating the effect of longer fennel fibres to improve the flexural strength of the tested bricks, as well as the long-term performances of tested products due to aging of the fennel particles contained in the used water. Moreover, a cost analysis will be done to evaluate the economic convenience of these bricks and a Life Cycle Assessment phase will be useful to quantify the energy spent for producing, using and dismantling the examined building products during their whole life. Results deriving from future research developments will be used to produce a new prototyping line able to generate a new type of green bricks for building constructions.

Author Contributions: Conceptualization, A.F.; methodology, A.F.; validation, A.F. and A.D.; formal analysis, A.F. and A.D.; investigation, A.F. and A.D.; resources, A.F.; data curation, A.D.; writing—original draft preparation, A.D.; writing—review and editing, A.F.; visualization, A.F. and A.D.; supervision, A.F.; project administration, A.F. All authors have read and agreed to the published version of the manuscript.

Funding: This research was financed by the Fenny srl company, with registered office in San Marzano sul Sarno (district of Salerno, Italy).

Data Availability Statement: Data deriving from the current study can be provided to the readers based upon their explicit request.

Acknowledgments: The authors thank the Fenny srl company for the financial support of the current research activity. In addition, the organizational support of the tests of Eng. Antonio Granatino, from the Agrosistemi Srl company, is gratefully acknowledged. A sincere acknowledgment goes similarly to the companies Kerakoll (in the person of Eng. Fulvio Bruno), Fassa Bortolo and Malvin (in the

person of Eng. Antonio Vittorioso) for the kind provision of the pre-mixed types used in the current research. Finally, a special thank is devoted to the Innovacustica srl company, in the person of Eng. Marco Anniciello, for the execution of acoustic tests on the studied building products.

Conflicts of Interest: The authors declare no conflict of interest.

References

1. Eurostat. Generation of Waste by Waste Category, Hazardousness and NACE Rev 2 Activity. Available online: https://ec.europa.eu/eurostat/web/products-datasets/-/ENV_WASGEN (accessed on 1 July 2021).
2. Keeler, M.; Burke, B. *Fundamentals of Integrated Design for Sustainable Building*; John Wiley & Sons, Inc.: Hoboken, NJ, USA, 2009.
3. Huang, B.; Wang, X.; Kua, H.; Geng, Y.; Bleischwitz, R.; Ren, J. Construction and demolition waste management in China through the 3r principle. *Resour. Conserv. Recycl.* **2018**, *129*, 36–44. [[CrossRef](#)]
4. Heravi, G.; Fathi, M.; Faeghi, S. Multi-criteria group decision-making method for optimal selection of sustainable industrial building options focused on petrochemical projects. *J. Clean. Prod.* **2017**, *142*, 2999–3013. [[CrossRef](#)]
5. Birgisdóttir, H.; Rasmussen, F.N. *Introduction to LCA of Buildings*, 1st ed.; Danish Transport and Construction Agency: Copenhagen, Denmark, 2016.
6. Sanal, I.; Verma, D. Construction Materials Reinforced with Natural Products. In *Handbook of Ecomaterials*; Martínez, L., Kharissova, O., Kharisov, B., Eds.; Springer: Cham, Switzerland, 2017. [[CrossRef](#)]
7. The Worldwatch Institute. *Annual Report*; The Worldwatch Institute: Washington, DC, USA, 2006.
8. Maziz, A.; Tarfaoui, M.; Gemi, L.; Rechak, S.; Nachtane, M. A progressive damage model for pressurized filament-wound hybrid composite pipe under low-velocity impact. *Compos. Struct.* **2021**, *276*, 114520. [[CrossRef](#)]
9. Gemi, D.S.; Şahin, Ö.S.; Gemi, L. Experimental investigation of the effect of diameter upon low velocity impact response of glass fiber reinforced composite pipes. *Compos. Struct.* **2021**, *275*, 114428. [[CrossRef](#)]
10. Ivens, J.; Urbanus, M.; De Smet, C. Shape recovery in a thermoset shape memory polymer and its fabric-reinforced composites. *Express Polym. Lett.* **2011**, *5*, 254–261. [[CrossRef](#)]
11. Korotkov, R.; Vedernikov, A.; Gusev, S.; Alajarmeh, O.; Akhatov, I.; Safonov, A. Shape memory behavior of unidirectional pultruded laminate. *Compos. Part A Appl. Sci. Manuf.* **2021**, *150*, 106609. [[CrossRef](#)]
12. Vedernikov, A.; Safonov, A.; Tucci, F.; Carlone, P.; Akhatov, I. Pultruded materials and structures: A review. *J. Compos. Mater.* **2020**, *54*, 4081–4117. [[CrossRef](#)]
13. Yu, T.; Zhang, Z.; Song, S.; Bai, Y.; Wu, D. Tensile and flexural behaviors of additively manufactured continuous carbon fiber-reinforced polymer composites. *Compos. Struct.* **2019**, *225*, 111147. [[CrossRef](#)]
14. Czapski, P.; Jakubczak, P.; Bienias, J.; Urbaniak, M.; Kubiak, T. Influence of autoclaving process on the stability of thin-walled, composite columns with a square cross-section—Experimental and numerical studies. *Compos. Struct.* **2020**, *250*, 112594. [[CrossRef](#)]
15. Mekonnen, M.M.; Hoekstra, A.Y. *National Water Footprint Accounts: The Green, Blue and Grey Water Footprint of Production and Consumption*; UNESCO-IHE Institute for Water Education: Delft, The Netherlands, 2011.
16. De Jong, C.; Lawler, D.; Essery, R. Mountain hydroclimatology and snow seasonality and hydrological change in mountain environments. *Hydrol. Process.* **2009**, *23*, 955–961. [[CrossRef](#)]
17. Viviroli, D.; Dürr, H.H.; Messerli, B.; Meybeck, M.; Weingartner, R. Mountains of the world, water towers for humanity: Typology, mapping, and global significance. *Water Resour. Res.* **2007**, *43*, 1–13. [[CrossRef](#)]
18. Messerli, B.; Viviroli, D.; Weingartner, R. Mountains of the world—Vulnerable water towers for the 21st century. *Ambio Spec. Rep.* **2004**, *13*, 29–34. [[CrossRef](#)]
19. U.S. Department of Agriculture Agricultural Research Service. Composition of Foods. Raw, Processed, Prepared. USDA National Nutrient Database for Standard Reference, Release 23. Available online: https://www.ars.usda.gov/ARSUserFiles/80400535/DATA/sr23/sr23_doc.pdf (accessed on 1 July 2021).
20. Al-Snafi, A.E. The chemical constituents and pharmacological effects of *Foeniculum vulgare*—A review. *IOSR J. Pharm.* **2018**, *8*, 81–96.
21. Charles, D.J. Fennel. In *Antioxidant Properties of Spices, Herbs and Other Sources*; Springer: New York, NY, USA, 2012; pp. 287–293. [[CrossRef](#)]
22. Bokaie, M.; Farajkhoda, T.; Enjezab, B.; Khoshbin, A.; Karimi-Zarchi, M. Oral fennel (*Foeniculum vulgare*) drop effect on primary dysmenorrhea: Effectiveness of herbal drug. *Iran J. Nurs. Midwifery Res.* **2013**, *18*, 128–132. [[PubMed](#)]
23. Choi, E.M.; Hwang, J.K. Antiinflammatory, analgesic and antioxidant activities of the fruit of *Foeniculum vulgare*. *Fitoterapia* **2004**, *75*, 557–565. [[CrossRef](#)] [[PubMed](#)]
24. De Marino, S.; Gala, F.; Borbone, N.; Zollo, F.; Vitalini, S.; Visioli, F.; Iorizzi, M. Phenolic glycosides from *Foeniculum vulgare* fruit and evaluation of antioxidative activity. *Phytochemistry* **2007**, *68*, 1805–1812. [[CrossRef](#)]
25. Uslu, Ö.S.; Gedik, O. A Research on the using of fennel hay as animal feed additive. In Proceedings of the 2nd International Conference on Agriculture, Technology, Engineering and Sciences (ICATES 2019), Lviv, Ukraine, 18–20 September 2019.
26. Pałka, S.; Kmiecik, M.; Migdał, L.; Siudak, Z. The effect of a diet containing fennel (*Foeniculum vulgare* Mill.) and goat's-rue (*Galega officinalis* L.) on litter size and milk yield in rabbits. *Sci. Ann. Pol. Soc. Anim. Prod.* **2019**, *4*, 73–78. [[CrossRef](#)]

27. Ahmad, B.S.; Talou, T.; Saad, Z.; Hijazi, A.; Cerny, M.; Kanaan, H.; Chokr, A.; Merah, O. Fennel oil and by-products seed characterization and their potential applications. *Ind. Crops Prod.* **2018**, *111*, 92–98. [[CrossRef](#)]
28. Haddar, W.; Elksibi, I.; Meksi, N.; Mhenni, M.F. Valorization of the leaves of fennel (*Foeniculum vulgare*) as natural dyes fixed on modified cotton: A dyeing process optimization based on a response surface methodology. *Ind. Crops Prod.* **2014**, *52*, 588–596. [[CrossRef](#)]
29. Barros, L.; Cavalho, A.M.; Ferreira, I.C.F.R. The nutritional composition of fennel (*Foeniculum vulgare*): Shoots, leaves, stems and inflorescences. *LWT Food Sci. Technol.* **2010**, *43*, 814–818. [[CrossRef](#)]
30. Mariniello, L.; Giosafatto, C.V.L.; Moschetti, G.; Aponte, M.; Masi, P.; Sorrentino, A.; Porta, R. Fennel waste-based films suitable for protecting cultivations. *Biomacromolecules* **2007**, *8*, 3008–3014. [[CrossRef](#)] [[PubMed](#)]
31. Lionetto, F.; Moscatello, A.; Totaro, G.; Raffone, M.; Maffezzoli, A. Experimental and numerical study of vacuum resin infusion of stiffened carbon fiber reinforced panels. *Materials* **2020**, *13*, 4800. [[CrossRef](#)] [[PubMed](#)]
32. Vedernikov, A.; Nasonov, Y.; Korotkov, R.; Gusev, S.; Akhatov, I.; Safonov, A. Effects of additives on the cure kinetics of vinyl ester pultrusion resins. *J. Compos. Mater.* **2021**, *55*, 2921–2937. [[CrossRef](#)]
33. EN 196-1:2016; Methods of Testing Cement—Part 1: Determination of Strength. European Committee for Standardization: Brussels, Belgium, 2016.
34. EN 12390-5:2019-08; Testing Hardened Concrete—Part 5: Flexural Strength of Test Specimens. European Committee for Standardization: Brussels, Belgium, 2019.
35. UNI EN 12390-3:2019; Testing Hardened Concrete—Part 3: Compressive Strength of Test Specimens. European Committee for Standardization: Brussels, Belgium, 2019.
36. UNI 11307:2008; Testing for Hardened Concrete—Shrinkage Determination. UNI Italian Committee for Standardization (Ente Nazionale Italiano di Unificazione): Milan, Italy, 2008.
37. UNI EN 13755:2008; Natural Stone Test Methods. Determination of Water Absorption at Atmospheric Pressure. European Committee for Standardization: Brussels, Belgium, 2008.
38. ASTM E2611-09; Standard Test Method for Measurement of Normal Incidence Sound Transmission of Acoustical Materials Based on the Transfer Matrix Method. ASTM International: West Conshohocken, PA, USA, 2009.
39. Hopper, C.; Assous, S.; Wilkinson, P.B.; Gunn, D.A.; Jackson, P.D.; Rees, J.G.; O’Leary, R.L.; Lovell, M.A. Bioinspired low-frequency material characterisation. *Adv. Acoust. Vib.* **2012**, *2012*, 927903. [[CrossRef](#)]